Team, 2013. R Foundation for Statistical Computing, Vienna, Austria. URL http://www.R-project.org/) with a package "coin". Hardy-Weinberg equilibrium was examined to compare the observed and expected genotype frequencies using a Chi-square test. Statistical significance of reporter experiments and gene expression analyses were analyzed using statistical softwares JMP version 10.0.2 and StatView version 5.0 software (SAS Institute Inc.).

Results

Database surveillance of SNPs of *EPAS1* in relation to its gene expression

Among the 3 Hap-tag SNPs (rs13419896, rs4953354, and rs4953388) that were implicated to contribute to the adaptation to high-altitude hypoxia in Sherpas [22], we found binding sites and binding activities for the C/EBP-β, AP-1 or MYC family of transcription factors in a number of cancer cell types in the region of the *EPAS1* rs13419896 locus within intron 1 of the gene by surveillance of ChIP-seq datasets from the ENCODE (S1 Fig). Interestingly enough, when analyzed the sequences using JASPAR Core Vertebrata, we found that relative scores, indices for probability of transcription factor binding, of C/EBP-β and AP-1 were affected by the rs13419896 SNP among the 3 transcription factors as mentioned above; C/EBP-β and AP-1 showed much higher scores of 0.842 and 0.855 in the sequence with *A* allele at rs13419896, respectively, than those with *G* allele (0.734 and 0.744). These data prompted us to examine the role of rs13419896 in regulation of the *EPAS1* gene expression.

The rs13419896 SNP altered the reporter gene activities

In order to test possible functional differences caused by the rs13419896 locus, we next prepared luciferase reporter constructs harboring the *EPAS1* fragment encompassing the rs13419896 locus in front of the minimum promoter (Fig 1A) and performed transient transfection analyses in A549, PC-9 and HSC-2 cancer cell lines. The constructs with the fragments containing the rs13419896 locus showed increased reporter activities as compared to the original reporter pGL4.26 in all the cell lines tested, regardless of the genotype of the SNP, suggesting that this short sequence within the intron 1 of *EPAS1* function as a transcriptional enhancer element ($P < 0.05$, Fig 1B–1D). Interestingly, the reporter construct containing the fragment with the *A* allele of rs13419896 (pGL4.26-EPAS1-A) showed significantly higher activity than one with the *G* allele (pGL4.26-EPAS1-G) in all the cell lines tested ($P < 0.01$, $P < 0.05$ as shown in Fig 1B–1D), suggesting that the enhancer activity of this regulatory element is affected by the genotype of the rs13419896 SNP.

Since the rs13419896 SNP was implicated to alter binding affinities of AP-1 and C/EBP-β by the aforementioned bioinformatics analysis, we next performed co-transfection experiments in A549 cells to evaluate the effects of overexpressing AP-1, c-MYC, or C/EBP-β transcription factors on the reporter activities. Surprisingly, forced expression of c-Jun or c-FOS, components of the transcription factor AP-1, significantly increased the reporter activity of only pGL4.26-EPAS1-A but not that of pGL4.26-EPAS1-G (Fig 2A and 2B). On the other hand, C/EBP-β increased the transcriptional activity of both of the reporter constructs with similar amplitude, while c-Myc did not show significant alterations in the activity of both constructs.

Comparison of expression levels of *EPAS1* mRNA and protein in cancer cell lines by the rs13419896 SNP

In order to explorer effects of the rs13419896 SNP on endogenous gene expression levels of the *EPAS1*, we genotyped the SNP and evaluated levels of the gene expression in diverse cancer cell

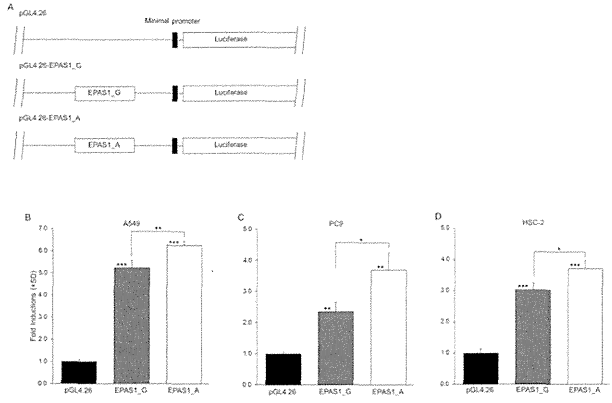

Fig 1. *EPAS1* SNP luciferase reporter activities in cancer cell lines. (A) Schematic representation of luciferase reporter constructs with different *EPAS1* SNP alleles as shown. Short fragments containing the *EPAS1* SNP locus (rs13419896) were subcloned into the pGL4.26 minimal promoter luciferase reporter plasmid. (B-D) Bar charts show luciferase reporter activity after transient transfection experiments in A549 (B), PC9 (C), and HSC-2 (D) cells. Luciferase reporter activity was calculated as a ratio to Renilla luciferase activity generated by the pRL-SV40 co-transfection control. Each value represents the mean + standard deviation (SD) for at least three independent experiments. *P*-values were calculated using Student's *t*-test with *: $P < 0.05$, **: $P < 0.01$ and ***: $P < 0.0001$.

doi:10.1371/journal.pone.0134496.g001

lines. When the cells were divided into two groups by presence or absence of the *A* allele at the rs13419896 locus, cancer cells with the *A* allele of the rs13419896 demonstrated significantly higher *EPAS1* gene expression levels than for any others without the *A* allele ($P = 0.022$, Welch's *t* test)(Fig 3A). We further analyzed levels of EPAS1 (HIF-2α) protein expression in

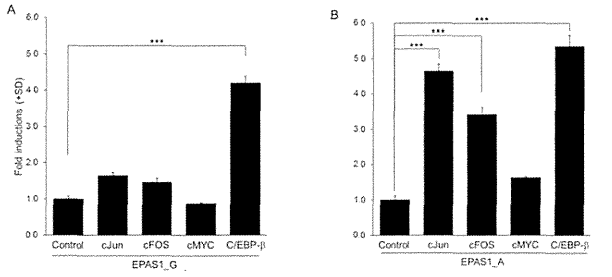

Fig 2. Effects of database-suggested transcription factors on rs13419896 SNP luciferase reporter activities. (A and B) To evaluate the effects of overexpressing AP-1 (c-Jun and c-FOS), MYC, or C/EBP-β transcription factors on rs13419896 SNP luciferase reporter activity, co-transfection experiments were performed in A549 lung adenocarcinoma cells. Bar charts show luciferase reporter activity of pGL4.26-EPAS1-G (A) or pGL4.26-EPAS1-A (B). Luciferase reporter activity was calculated as a ratio to Renilla luciferase activity generated by the pRL-SV40 co-transfection control. Each value represents the mean + standard deviation (SD) for at least three independent experiments. *P*-values were calculated using Dunnett's test with ***: $P < 0.0001$.

doi:10.1371/journal.pone.0134496.g002

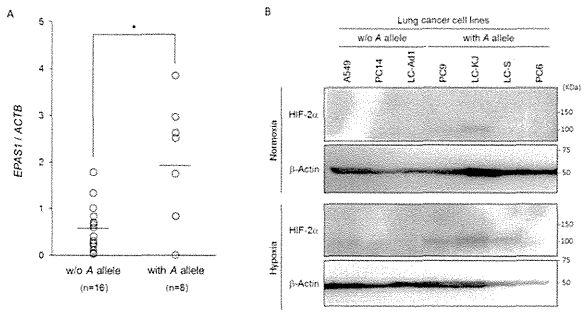

Fig 3. Expression levels of *EPAS1* mRNA in cancer cell lines by the rs13419896 SNP. (A) The *EPAS1* gene expression levels evaluated by real-time RT-PCR were compared between cancer cells' groups by rs13419896 status; one with the *A* allele at the SNP site (with *A* allele) and others without (w/o *A* allele). The expression levels of *EPAS1* in each cell line was calculated as a ratio to that of *ACTB* and each value represents the mean for at least three independent experiments (open circle). Each bar indicates average of expression level in each group. *P*-values were calculated using Welch's *t* test with *: $P = 0.022$. (B) The EPAS1 protein expression levels were compared between genotypes as above. Several lung cancer cell lines were incubated under normoxic (21% pO_2) or hypoxic (1% pO_2) for 24 hours. Whole cell extracts prepared from each cell line were subjected in immunoblotting analysis using anti-EPAS1 (HIF-2α) or anti-β-actin as a control.

doi:10.1371/journal.pone.0134496.g003

several lung cancer cell lines by immunoblotting analyses. As results, EPAS1 proteins were detected in PC9 and LC-KJ with the *A* allels even under normoxic conditions and were obviously increased in some of hypoxic cancer cells, A549, PC9, LC-KJ, and LC-S (Fig 3B).

The A allele of rs13419896 SNP of *EPAS1* was associated with poor overall survival of non-small cell lung cancer patients

Since the rs13419896 SNP was suggested to link with enhanced expression of *EPAS1* gene, we then explored possible associations of the SNP with clinicopathological factors of Japanese NSCLC patients. Genotypes of the rs13419896 SNP were determined in 76 NSCLC patients, and found to be in good agreement with Hardy-Weinberg equilibrium ($P = 0.45$, Chi-square test, Table 2). No significant difference was found amongst genotype frequencies between the Japanese NSCLC samples in this study and the healthy Japanese population of the HapMap project ($P = 0.94$, extended Fisher's exact test, Table 2). We then examined the relationship between the *EPAS1* SNPs and various clinicopathological characteristics (Table 3). The frequency of minor allele of rs13419896 tended to be higher in females than in males: A frequency of patients possessing at least one *A* allele of rs13419896 (*A/A* or *A/G* genotype) were 70.0% (14 of 20) in females and 44.6% (25 of 56) in males, though this was not statistically significant ($P = 0.07$, Fisher's exact test). In addition, distribution of differentiation tended to differ by the SNP with a marginal significance ($P = 0.06$, extended Fisher's exact test). Other than the gender and differentiation, we did not find any statistical associations of the SNP with clinicopathological characteristics including age, histology, tumor size, and stage.

We then assessed association of the rs13419896 SNP with overall survival for the NSCLC. The median survival time of patients with at least one *A* allele of rs13419896 (*A/A* or *A/G*) was significantly shorter than that with the *G/G* homozygote (28.0 months vs. 52.5 months, $P = 0.047$, log-rank test, Fig 4). When compared cumulative survival rates at 12, 24, and 48

Table 2. Genotype frequencies of the EPAS1 rs13419896 SNP in Japanese NSCLC patients with those in HapMap-JPT.

Genotype	NSCLC		HapMap-JPT[a]		P^b
	n	%	n	%	
G/G	37	48.7	52	46.0	0.94
A/G	30	39.5	46	40.7	
A/A	9	11.8	15	13.3	
G allele	104	68.4	150	66.4	0.74
A allele	48	31.6	76	33.6	

[a]http://hapmap.ncbi.nlm.nih.gov/cgi-perl/snp_details_phase3?name = rs13419896&source = hapmap28_B36&tmpl = snp_details_phase3

[b](*Extended*) *Fisher's exact test*

doi:10.1371/journal.pone.0134496.t002

months, patients with the *G/G* homozygote showed much higher rates than those with *A/G* or *A/A* genotype at 12 and 48 months ($P = 0.009$ and 0.004, respectively) (S1 Table). A multivariate analysis of the 74 NSCLC patients (2 patients were excluded because of the lack of tumor size data) using a Cox proportional hazard model demonstrated that the possession of *A* allele (*A/G* or *A/A* genotype) of rs13419896, along with clinical stage, was an independent variable for risk estimation of overall survival for NSCLC patients [hazard ratio (HR) = 2.31, 95% CI = 1.14–4.81, $P = 0.021$], after adjustment for age, gender, stage, histology, tumor size, and differentiation.

Table 3. Associations of various clinicopathological factors with *EPAS1* rs13419896 polymorphism in NSCLC patients.

		rs13419896		
		G/G	*A/G or A/A*	*P*
Mean Age (yr)		65.0	66.6	0.41
(SD)		7.7	8.6	
Gender (n)	Male (%)	31 (40.8)	25 (32.9)	0.07
	Female (%)	6 (7.9)	14 (18.4)	
Histology (n)	Adenocarcinoma (%)	20 (26.3)	23 (30.3)	0.93
	Adenosquamous Carcinoma (%)	2 (2.6)	2 (2.6)	
	Squamous Cell Carcinoma (%)	15 (19.8)	14 (18.4)	
Stage (n)	I (%)	16 (21.1)	15 (19.7)	0.13
	II (%)	6 (7.9)	1 (1.3)	
	III (%)	11 (14.5)	14 (18.4)	
	IV (%)	4 (5.3)	9 (11.8)	
Differentiation (n)	Well (%)	5 (6.6)	13 (17.1)	0.06
	Moderately (%)	16 (21.0)	19 (25.0)	
	Poorly (%)	13 (17.1)	6 (7.9)	
	NA[b] (%)	3 (4.0)	1 (1.3)	
Mean tumor size[a] (cm)		3.9	4.4	0.20
(SD)		1.5	1.7	

[a]Two cases were missing for the data of tumor size.

[b]NA, not applicable.

doi:10.1371/journal.pone.0134496.t003

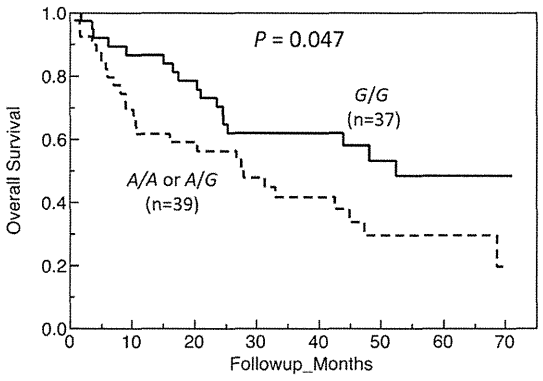

Fig 4. Overall survival of NSCLC patients by the rs13419896 SNP in *EPAS1*. Kaplan-Meier survival plots stratified according to genotypes of rs13419896 are shown. Difference in overall survival across genotypic groups of NSCLC patients was examined using the log-rank test with *P*-values as indicated.

doi:10.1371/journal.pone.0134496.g004

Discussion

Recently, several SNPs of *EPAS1* have been shown to correlate with the development of various diseases such as osteoarthritis [16], retinopathy of prematurity [17], maximum metabolic power in elite endurance athletes [18], physiologic adaptation in high altitude populations [19–22], and susceptibility towards renal cell carcinoma (RCC) and prostate cancer [23, 24]. However, a mechanistic link between these SNPs and gene expression levels of the *EPAS1* has scarcely been known, except for the rs17039192 located in the 5'-untranslated region, that gave altered promoter activities in reporter gene assay in chondrogenic cells [16].

In this study, bioinformatic analyses prompted us to test a role of one of the Hap-tag SNPs, rs13419896 located within intron1 of the gene, in regulation of *EPAS1* expression. In fact, we found that a fragment in the intron 1 of *EPAS1* contains transcriptional regulatory elements and nucleotide difference at the rs13419896 locus may functionally affect enhancer activities in cancer cell lines. Interestingly, further co-transfection experiments strongly indicated that AP-1 transcription factor might be involved in the differential transcriptional activities between the rs13419896 alleles. The observed specific transactivation by exogenous AP-1 components only in constructs with *A* allele at the rs13419896 agreed well with the higher relative score for AP-1 with *A* allele at the SNP as shown by JASPAR Core Vertebrata analysis. Previously, overexpression of c-Jun and c-Fos proteins was observed in 31–50 and 60%, respectively, of NSCLC tissues [34, 35]. The overexpressed c-Jun or c-Fos may transactivate the *EPAS1* gene expression *via*, at least in part, an enhancer element within intron 1 of the gene in an allele-specific manner at the rs13419896 locus. This was also supported by the observation of gene and protein expression levels of *EPAS1* by the rs13419896 SNP in various cancer cells. Although we did not completely confirm the genotypes (including allelic loss, amplification, or mutations) of the cancer cell lines tested, we found that the cells with *A* allele at rs13419896 of *EPAS1* showed significantly higher *EPAS1* gene and protein expression levels compared with those lacking *A* allele regardless of differences in genetic background. Taken together these data, it is strongly suggested that the *A* allele at rs13419896 SNP of *EPAS1* plays an important role in alteration of binding affinity of AP-1, resulting in differentiated levels of expression of the EPAS1 in NSCLC tissue.

The observed association of the *A* allele of the rs13419896 SNP with increased expression levels of EPAS1 inspired us to further examine the possible role of the SNP in prognosis of Japanese NSCLC patients, since overexpression of EPAS1 was reported to be associated with a poor prognosis. We demonstrated for the first time that the rs13419896 locus was an independent variable for risk estimation of overall survival of NSCLC.

In human NSCLC, overexpression of HIF-2α (EPAS1) was consistently associated with histology as SCC being dominant, increased tumor size, and angiogenesis, resulting in worse prognosis and decreased survival rates [13, 14]. In our study, we did not find any association of the rs13419896 SNP with histology and tumor size. On the other hand, the hazard ratio of possession of *A* allele over the *G* allele in Cox's hazard model was 2.31, that is comparable to the ratio of high expression of HIF-2α obtained previously (2.01 and 1.71) [13, 14]. Recent meta-analysis examining overall survival by the overexpression of HIF-2α protein also demonstrated HR of 2.02 (95%CI: 1.47–2.77) [36]. Considering these, the rs13419896 SNP may be one of the important factors that contribute to the overexpression of HIF-2α in NSCLC tissue and thus be a useful prognostic marker for NSCLC. We observed a statistically significant difference of cumulative survival rate between patients with *A* allele and without at 12 months post operation (S1 Table). If our observation is confirmed by other cohorts in future, genotyping of the SNP may become clinically important for considering patients' care and counseling immediately. Besides NSCLC, other cancers such as colorectal and head and neck cancers were also reported to show a poor prognosis with overexpression of the HIF-2α in meta-analyses [37, 38]. Since overexpression of AP-1 components can be observed for these cancers [39, 40], the rs13419896 SNP may contribute to the overexpression of HIF-2α and be a useful prognostic marker in various cancers.

In conclusion, we found here for the first time that nucleotide difference at the rs13419896 SNP may affect *EPAS1* gene and protein expression, specifically in response to AP-1, and that the *A* allele of *EPAS1* SNP is associated with poorer prognosis of lung cancer patients. To establish the *EPAS1* SNP as a useful clinical prognostic marker and to further clarify their molecular mechanisms, larger scale clinicopathological studies of lung cancer and/or other types of cancer will provide additional insights into these aspects.

Supporting Information

S1 Fig. UCSC Genome Browser representation of ENCODE Consortium ChIP-Seq data for transcription factor binding overlaid on human genome build hg19. Top panels show genomic structure of the *EPAS1* gene compiled from UCSC, RefSeq and GenBank with thick bars indicating exonic coding sequences, thin bars showing non-coding exon regions (5' and 3' UTRs) and arrows denoting introns with 5' to 3' directionality. The horizontal axis shows genome position in bp in the interval from chr2: 46,514,938–46,626,784. The position of the rs13419896 SNP is indicated in red and its relative position is extrapolated across all datasets as a broken blue line. ChIP-Seq data is shown in the same genome location with the vertical axis indicating ChIP enrichment of transcription factor binding for CEBPB (black), MYC (red), FOS (green), JUN (blue), JUNB (violet) and JUND (orange) in the specified cell lines. Scale bar indicates genomic distance of 50 kb.
(PDF)

S1 Table. Comparisons of cumulative survival rates between patients with genotypes *G/G* and *A/G* or *A/A*.
(DOCX)

Acknowledgments

The authors thank Prof. N. Kohno, Emeritus Prof. K. Inai (Hiroshima University), Prof. F. Yunus and Dr. E. Syahruddin (University of Indonesia) for their kind support and encouragement. We also thank Ms. C. Oda for her technical assistance. Part of this work was carried out at the Analysis Center of Life Science, Hiroshima University.

Author Contributions

Conceived and designed the experiments: HE KT. Performed the experiments: ACP YY EG KT. Analyzed the data: HE KLL LP KT. Contributed reagents/materials/analysis tools: TI MN KH. Wrote the paper: HE KT.

References

1. Tanimoto K, Yoshiga K, Eguchi H, Kaneyasu M, Ukon K, Kumazaki T, et al. Hypoxia-inducible factor-1α polymorphisms associated with enhanced transactivation capacity, implying clinical significance. Carcinogenesis. 2003; 24:1779–1783. PMID: 12919954
2. Semenza GL. Defining the role of hypoxia-inducible factor 1 in cancer biology and therapeutics. Oncogene. 2010; 29:625–634. doi: 10.1038/onc.2009.441 PMID: 19946328
3. Patel SA, Simon MC. Biology of hypoxia-inducible factor-2α in development and disease. Cell death differ. 2008; 15:628–634. doi: 10.1038/cdd.2008.17 PMID: 18259197
4. Putra AC, Tanimoto K, Arifin M, Hiyama K. Hypoxia-inducible factor-1α polymorphisms are associated with genetic aberrations in lung cancer. Respirology. 2011; 16:796–802. doi: 10.1111/j.1440-1843.2011.01972.x PMID: 21435097
5. Lofstedt T, Fredlund E, Holmquist-Mengelbier L, Pietras A, Ovenberger M, Poellinger L, Påhlman S. Hypoxia inducible factor-2α in cancer. Cell Cycle. 2007; 6:919–926. PMID: 17404509
6. Acker T, Plate KH. A role for hypoxia and hypoxia-inducible transcription factors in tumor physiology. J. Mol. Med. (Berl). 2002; 80:562–575.
7. Rankin EB, Giaccia AJ. The role of hypoxia-inducible factors in tumorigenesis. Cell death differ. 2008; 15:678–685. doi: 10.1038/cdd.2008.21 PMID: 18259193
8. Hansen AE, Kristensen AT, Law I, Jorgensen JT, Engelholm SA. Hypoxia-inducible factors—regulation, role and comparative aspects in tumourigenesis. Vet. Comp. Oncol. 2011; 9:16–37. doi: 10.1111/j.1476-5829.2010.00233.x PMID: 21303451
9. Wiesener MS, Jurgensen JS, Rosenberger C, Scholze CK, Horstrup JH, Warnecke C, et al. Widespread hypoxia-inducible expression of HIF-2α in distinct cell populations of different organs. FASEB J. 2003; 17:271–273. PMID: 12490539
10. Groenman F, Rutter M, Caniggia I, Tibboel D, Post M. Hypoxia-inducible factors in the first trimester human lung. J. Histochem. Cytochem. 2007; 55:355–363. PMID: 17189520
11. Kim WY, Perera S, Zhou B, Carretero J, Yeh JJ, Heathcote SA, et al. HIF2α cooperates with RAS to promote lung tumorigenesis in mice. J. Clin. Invest. 2009; 119:2160–2170. PMID: 19662677
12. Mazumdar J, Hickey MM, Pant DK, Durham AC, Sweet-Cordero A, Vachani A, et al. HIF-2α deletion promotes Kras-driven lung tumor development. Proc. Natl. Acad. Sci. U.S.A. 2010; 107:14182–14187. doi: 10.1073/pnas.1001296107 PMID: 20660313
13. Wu XH, Qian C, Yuan K. Correlations of hypoxia-inducible factor-1α/hypoxia-inducible factor-2α expression with angiogenesis factors expression and prognosis in non-small cell lung cancer. Chin. Med. J. (Engl.). 2011; 124:11–18.
14. Giatromanolaki A, Koukourakis MI, Sivridis E, Turley H, Talks K, Pezzella F, et al. Relation of hypoxia inducible factor 1 alpha and 2 alpha in operable non-small cell lung cancer to angiogenic/molecular profile of tumours and survival. Br. J. Cancer. 2011; 85:881–890.
15. Han SS, Yeager M, Moore LE, Wei MH, Pfeiffer R, Toure O, et al. The chromosome 2p21 region harbors a complex genetic architecture for association with risk for renal cell carcinoma. Hum. Mol. Genet. 2011; 21:1190–1200. doi: 10.1093/hmg/ddr551 PMID: 22113997
16. Saito T, Fukai A, Mabuchi A, Ikeda T, Yano F, Ohba S, et al. Transcriptional regulation of endochondral ossification by HIF-2α during skeletal growth and osteoarthritis development. Nat. Med. 2010; 16:678–686. doi: 10.1038/nm.2146 PMID: 20495570

17. Mohamed S, Schaa K, Cooper ME, Ahrens E, Alvarado A, Colaizy T, et al. Genetic contributions to the development of retinopathy of prematurity. Pediatr. Res. 2009; 65:193–197. doi: 10.1203/PDR.0b013e31818d1dbd PMID: 18787502

18. Henderson J, Withford-Cave JM, Duffy DL, Cole SJ, Sawyer NA, Gulbin JP, et al. The EPAS1 gene influences the aerobic-anaerobic contribution in elite endurance athletes. Hum Genet. 2005; 118:416–423. PMID: 16208515

19. Beall CM, Cavalleri GL, Deng L, Elston RC, Gao Y, Knight J, et al. Natural selection on EPAS1 (HIF2α) associated with low hemoglobin concentration in Tibetan highlanders. Proc. Natl. Acad. Sci. U.S.A. 2010; 107:11459–11464. doi: 10.1073/pnas.1002443107 PMID: 20534544

20. Yi X, Liang Y, Huerta-Sanchez E, Jin X, Cuo ZX, Pool JE, et al. Sequencing of 50 human exomes reveals adaptation to high altitude. Science. 2010; 329:75–78. doi: 10.1126/science.1190371 PMID: 20595611

21. Peng Y, Yang Z, Zhang H, Cui C, Qi X, Luo X, et al. Genetic variations in Tibetan populations and high-altitude adaptation at the Himalayas. Mol. Biol. Evol. 2011; 28:1075–1081. doi: 10.1093/molbev/msq290 PMID: 21030426

22. Hanaoka M, Droma Y, Basnyat B, Ito M, Kobayashi N, Katsuyama Y, et al. Genetic variants in EPAS1 contribute to adaptation to high-altitude hypoxia in Sherpas. PLOS One. 2012; 7:e50566. doi: 10.1371/journal.pone.0050566 PMID: 23227185

23. Purdue MP, Johansson M, Zelenika D, Toro JR, Scelo G, Moore LE, et al. Genome-wide association study of renal cell carcinoma identifies two susceptibility loci on 2p21 and 11q13.3. Nat. Genet. 2011; 43:60–65. doi: 10.1038/ng.723 PMID: 21131975

24. Ciampa J, Yeager M, Amundadottir L, Jacobs K, Kraft P, Chung C, et al. Large-scale Exploration of Gene-Gene Interactions in Prostate Cancer Using a Multistage Genome-wide Association Study. Cancer Res. 2011; 71:3287–3295. doi: 10.1158/0008-5472.CAN-10-2646 PMID: 21372204

25. Mathelier A, Zhao X, Zhang AW, Parcy F, Worsley-Hunt R, Arenillas DJ, et al. JASPAR 2014: an extensively expanded and updated open-access database of transcription factor binding profiles. Nucleic Acids Res. 2014; 42(Database issue):D142–147. doi: 10.1093/nar/gkt997 PMID: 24194598

26. Mendoza C, Sato H, Hiyama K, Ishioka S, Isobe T, Maeda H, et al. Allelotype and loss of heterozygosity around the L-myc gene locus in primary lung cancers. Lung Cancer. 2000; 28:117–125. PMID: 10717329

27. Arifin M, Hiyama K, Tanimoto T, Wiyono WH, Hiyama E, Nishiyama M. EGFR activating aberration occurs independently of other genetic aberrations or telomerase activation in adenocarcinoma of the lung. Oncol. Rep. 2007; 17:1405–1411. PMID: 17487398

28. Tanaka T, Tanimoto K, Otani K, Satoh K, Ohtaki M, Yoshida K, et al. Concise prediction models of anticancer efficacy of 8 drugs using expression data from 12 selected genes. Int. J. Cancer. 2004; 111:617–626. PMID: 15239142

29. Noguchi T, Tanimoto K, Shimokuni T, Ukon K, Tsujimoto H, Fukushima M, et al. Aberrant Methylation of Dihydropyrimidine Dehydrogenase Gene (DPYD) promoter, DPYD Expression, and Cellular Sensitivity to 5-fluorouracil in Cancer Cells. Clin. Cancer Res. 2004; 10:7100–7107. PMID: 15501990

30. Nakamura H, Tanimoto K, Yunokawa M, Kawamoto T, Kato Y, Yoshiga K, et al. Human mismatch repair gene, *MLH1*, is transcriptionally repressed by the hypoxia-inducible transcription factors, DEC1 and DEC2. Oncogene. 2008; 27:4200–4209. doi: 10.1038/onc.2008.58 PMID: 18345027

31. Oridate N, Nishi S, Inuyama Y, Sakai M. Jun and Fos related gene products bind to and modulate the GPE I, a strong enhancer element of the rat glutathione transferase P gene. Biochim. Biophys. Acta. 1994; 1219:499–504. PMID: 7918648

32. Arifin M, Tanimoto K, Putra AC, Hiyama E, Nishiyama M, Hiyama K. Carcinogenesis and cellular immortalization without persistent inactivation of p16/Rb pathway in lung cancer. Int. J. Oncol. 2010; 36:1217–1227. PMID: 20372796

33. Sobin LH, Hermanek P, Hutter RV TNM classification of malignant tumors. A comparison between the new (1987) and the old editions. Cancer. 1988; 61:2310–2314. PMID: 3284634

34. Szabo E, Riffe ME, Steinberg SM, Birrer MJ, Linnoila RI. Altered cJUN expression: an early event in human lung carcinogenesis. Cancer Res. 1996; 56:305–315. PMID: 8542585

35. Wodrich W, Volm M. Overexpression of oncoproteins in non-small cell lung carcinomas of smokers. Carcinogenesis. 1993; 14:1121–1124. PMID: 8389672

36. Li C, Lu HJ, Na FF, Deng L, Xue JX, Wang JW, et al. Prognostic role of hypoxic inducible factor expression in non-small cell lung cancer: a meta-analysis. Asian Pac J Cancer Prev. 2013; 14:3607–3612. PMID: 23886153

37. Chen Z, He X, Xia W, Huang Q, Zhang Z, Ye J, et al. Prognostic value and clinicopathological differences of HIFs in colorectal cancer: evidence from meta-analysis. PLoS One. 8(2013):e80337.

38. Gong L, Zhang W, Zhou J, Lu J, Xiong H, Shi X, et al. Prognostic value of HIFs expression in head and neck cancer: a systematic review. PLoS One. 2013; 8:e75094. doi: 10.1371/journal.pone.0075094 PMID: 24058651

39. Zhang W, Hart J, McLeod HL, Wang HL. Differential expression of the AP-1 transcription factor family members in human colorectal epithelial and neuroendocrine neoplasms. Am J Clin Pathol. 2005; 124:11–19. PMID: 15923159

40. Mishra A, Bharti AC, Saluja D, Das BC. Transactivation and expression patterns of Jun and Fos/AP-1 super-family proteins in human oral cancer. Int J Cancer. 2010; 126:819–829. doi: 10.1002/ijc.24807 PMID: 19653276

Cancer Immunol Immunother (2015) 64:1407–1417
DOI 10.1007/s00262-015-1742-0

ORIGINAL ARTICLE

Immunosuppressive activity of cancer-associated fibroblasts in head and neck squamous cell carcinoma

Hideyuki Takahashi[1] · Koichi Sakakura[1] · Reika Kawabata-Iwakawa[2] · Susumu Rokudai[3] · Minoru Toyoda[1] · Masahiko Nishiyama[3] · Kazuaki Chikamatsu[1]

Received: 8 January 2015 / Accepted: 10 July 2015 / Published online: 23 July 2015

Abstract Cancer-associated fibroblasts (CAFs) have been shown to play an important role in angiogenesis, invasion, and metastasis. In the present study, we determined whether CAFs within the tumor microenvironment (TME) in head and neck squamous cell carcinoma (HNSCC) contributed to promoting immunosuppression and evasion from immune surveillance. Six pairs of CAFs and normal fibroblasts (NFs) were established from the resected tumor tissues of patients with HNSCC. The effects of CAFs and NFs on the functions of T cells were comparatively analyzed. CAFs expressed the co-regulatory molecules, B7H1 and B7DC, whereas NFs did not. The expression levels of cytokine genes, including those for *IL6*, *CXCL8*, *TNF*, *TGFB1*, and *VEGFA*, were higher in CAFs. T cell proliferation was suppressed more by CAFs or their supernatants than by NFs. Moreover, PBMCs co-cultured with the supernatants of CAFs preferentially induced T cell apoptosis and regulatory T cells over those co-cultured with the supernatants of NFs. A microarray analysis revealed that the level of genes related to the leukocyte extravasation and paxillin signaling pathways was higher in CAFs than in NFs. These results demonstrated that CAFs collaborated with tumor cells in the TME to establish an immunosuppressive network that facilitated tumor evasion from immunological destruction.

Keywords Cancer-associated fibroblasts · Head and neck squamous cell carcinoma · Immunosuppression · Regulatory T cells · T cell apoptosis

Abbreviations

7-ADD	7-Amino-actinomycin D
APC	Allophycocyanin
CAF	Cancer-associated fibroblast
CCL7	Chemokine ligand 7
CFSE	Carboxyfluorescein succinimidyl ester
Cy	Cyanine
FAP	Fibroblast activation protein
GAPDH	Glyceraldehyde-3-phosphate dehydrogenase
HGF	Hepatocyte growth factor
HNSCC	Head and neck squamous cell carcinoma
IGF	Insulin-like growth factor
IL	Interleukin
IPA	Ingenuity pathway analysis
MMP	Matrix metalloproteinase
NF	Normal fibroblast
NSCLC	Non-small cell lung cancer
SMA	Smooth muscle actin
TGF	Transforming growth factor
TME	Tumor microenvironment
Treg	Regulatory T cells
VEGF	Vascular endothelial growth factor

Introduction

Head and neck squamous cell carcinoma (HNSCC) is a fatal malignancy that accounts for approximately 650,000

✉ Kazuaki Chikamatsu
tikamatu@gunma-u.ac.jp

[1] Department of Otolaryngology-Head and Neck Surgery, Gunma University Graduate School of Medicine, 3-39-22, Maebashi, Gunma 371-8511, Japan

[2] Division of Integrate Oncology Research, Gunma University Initiative for Advanced Research, 3-39-22, Maebashi, Gunma 371-8511, Japan

[3] Department of Molecular Pharmacology and Oncology, Gunma University Graduate School of Medicine, 3-39-22, Maebashi, Gunma 371-8511, Japan

new patients every year. In spite of continual improvements in surgical techniques and the introduction of new chemotherapeutic agents and radiotherapy regimens, the five-year survival rate of HNSCC has remained unchanged for decades and is still 50 % [1, 2]. Therefore, further explorations of new therapeutic targets are needed in order to improve the prognosis and survival of patients with HNSCC.

Tumor tissue is composed not only of tumor cells, but also of various stromal cells, including fibroblasts, epithelial cells, endothelial cells, and immune cells, and these stroma cells contribute to tumor growth and progression. Recent findings revealed that cancer-associated fibroblasts (CAFs), one of the most abundant and active cellular components of the tumor stroma, played an important role in angiogenesis, invasion, and metastasis unlike normal fibroblasts (NFs) residing in healthy tissue [3–5].

The abundance of CAFs has been clinically correlated with poor prognosis in several malignancies, including lung [6] and colorectal cancers [7]. CAFs produce various cytokines and growth factors, such as transforming growth factor (TGF)-β, vascular endothelial growth factor (VEGF), interleukin (IL)-6 and IL-8, and insulin-like growth factor (IGF), and directly or indirectly influence the behavior of malignant cells through signaling pathways mediated by these molecules [8, 9]. Based on these findings, CAFs are considered to be active participants in the induction of immunosuppression and promotion of tumor evasion from immune surveillance. However, the immunological significance of CAFs in the tumor microenvironment (TME) is not yet fully understood.

Anti-tumor innate and adaptive immunity comprising the cancer immune surveillance network are generally designed to survey, recognize, and eliminate tumor cells. T cells predominantly orchestrate the host immune system, and the T cell infiltration of tumor lesions has been reported to correlate with improved prognoses in various types of cancers [10, 11]. However, anti-tumor immunity is often down-regulated with a developing tumor due to the expansion of regulatory T cells (Treg) as well as the production of immunosuppressive factors [12–14]. Thus, human tumors are known to employ various immunosuppressive mechanisms to evade the anti-tumor activities of immune cells, and tumor evasion from immunological destruction has recently emerged as one of the hallmarks of cancer [15].

In the present study, we investigated whether CAFs within the TME contributed to tumor evasion in HNSCC which are known to be highly immunosuppressive [16]. After establishing six pairs of CAFs and NFs from the resected tumor tissues of patients with HNSCC, we performed a comparative analysis of CAFs and NFs to evaluate their ability to regulate the functions of T cells. Our results have provided novel insights into immunosuppressive mechanisms in the TME and suggest that novel therapeutic approaches targeting CAFs may benefit patients with HNSCC.

Materials and methods

Patient samples

Tumor tissues and their normal counterparts were obtained from six newly diagnosed HNSCC patients (3 oral cavity cancer and 3 hypopharyngeal cancer patients) who underwent surgery at the Department of Otolaryngology, Head and Neck Surgery, Gunma University Hospital. The normal counterparts were defined by the non-cancerous region at least 2 cm away from the tumor margin. Patients received no anticancer drugs or radiotherapy before surgery. All tumors were obtained according to the protocol, which was approved by the Institutional Review Board of Gunma University. All patients provided written informed consent. The tissue was soaked in DMEM (Gibco, Grand Island, NY) supplemented with 1000 units/ml penicillin, 1000 μg/ml streptomycin, and 2.5 μg/ml fungizone (all reagents from Gibco) for 4 h, and then washed with DMEM supplemented with 10 % FCS, 100 units/ml penicillin, and 100 μg/ml streptomycin (henceforth referred to as "conditioned DMEM"). The tissue was sliced into 1- to 3-mm^3 pieces under sterile conditions. These fragments were transferred into a six-well plate with conditioned DMEM. Half of the medium was changed once or twice a week thereafter. After the sufficient outgrowth of cells, fibroblasts were removed by a treatment with TrypLE™ Express Enzyme (Gibco) and seeded into tissue culture flasks. They were analyzed by flow cytometry or real-time quantitative reverse transcription polymerase chain reaction (RT-PCR) after the sufficient outgrowth of cells. All CAFs and NFs used in this study were from less than 10 passages. Culture supernatants were collected from semi-confluent cultures 72 h after the medium was changed and then centrifuged and stored at −80 °C until use.

Peripheral blood mononuclear cells

Peripheral blood mononuclear cells (PBMCs) were prepared from healthy donor blood by density gradient centrifugation on a Ficoll-Paque PLUS (GE Healthcare, Pittsburgh PA). They were stored at −80 °C until use.

Flow cytometry analysis of primary fibroblast cultures

Fibroblasts were stained with the following mouse anti-human antibodies to define the expression of fibroblast surface markers, HLA molecules, or co-regulatory molecules:

phycoerythrin (PE)-CD11b/Mac-1, PE-CD34, PE-CD45, PE-CD90/Thy-1, PE-α-smooth muscle actin (α-SMA) (all reagents from R&D Systems, Minneapolis, MN), PE-HLA class I, PE-HLA-DR, PE-CD80/B7-1, PE-CD86/B7-2, PE-B7H1/PD-L1, PE-B7DC/PD-L2, or PE-B7H3 (all reagents from eBioscience, San Diego, CA), and fibroblast activation protein (FAP; unconjugated; R&D Systems). A PE-conjugated goat anti-mouse monoclonal antibody (mAb; BD Pharmingen) was used as a secondary antibody for FAP staining. A Cytofix/Cytoperm™ Kit (BD Bioscience, San Jose, CA) was used to perform intracellular staining for PE-α-SMA. Respective immunoglobulin G (IgG) isotype-matched controls (BD Bioscience) were used as negative controls. Flow cytometry was conducted using a FACSCalibur flow cytometer (BD Bioscience), and data analysis was performed with FlowJo software (TreeStar, Ashland, OR).

Real-time qRT-PCR

Total RNA was extracted using an RNeasy mini kit (Qiagen, Valencia, CA). Quantitative RT-PCR was performed in triplicate using a Power SYBR Green RNA-to-CT 1-Step Kit on an Applied Biosystems StepOne (Applied Biosystems, Foster City, CA). The melting curve was recorded at the end of every run to assess product specificity. Glyceraldehyde-3-phosphate dehydrogenase (*GAPDH*) was used as an internal control gene. Relative expression levels were determined by the $2^{-\Delta\Delta C_t}$ method, in which Ct represented the threshold cycle.

The PCR primers used in this study were as follows: *IL6* forward primer, 5′-AAGCCAGAGCTGTGCAGATGAGTA-3′, reverse primer, 5′-TGTCCTGCAGCCACTGGTTC-3′; *CXCL8* forward primer, 5′-GTGCAGAGGGTTGTGGAGAAGTTT-3′, reverse primer, 5′-TCACTGGCATCTTCACTGATTCTTG-3′; *IL10* forward primer, 5′-GAGATGCCTTCAGCAGAGTGAAGA-3′, reverse primer, 5′-AGGCTTGGCAACCCAGGTAAC-3′; *TNF* forward primer, 5′-TGCTTGTTCCTCAGCCTCTT-3′, reverse primer, 5′-CAGAGGGCTGATTAGAGAGAGGT-3′; *VEGFA* forward primer, 5′-ACTTCCCCAAATCACTGTGG-3′, reverse primer, 5′-GTCACTCACTTTGCCCCTGT-3′; *TGFB1* forward primer, 5′-AGCGACTCGCCAGAGTGGTTA-3′, reverse primer, 5′-GCAGTGTGTTATCCCTGCTGTCA-3′; *FOXP3* forward primer, 5′-GTTCACACGCATGTTTGCCTTC-3′, reverse primer, 5′-GCACAAAGCACTTGTGCAGACTC-3′, and *GAPDH* forward primer, 5′-GCACCGTCAAGGCTGAGAAC-3′; reverse primer, 5′-ATGGTGGTGAAGACGCCAGT-3′.

Carboxyfluorescein succinimidyl ester (CFSE)-based suppression assay

Healthy donor PBMCs were incubated with 1.5 μM CFSE (Molecular Probe/Invitrogen) for 15 min at 37 °C and quenched with ice-cold FBS. After 5 min at room temperature in the dark, they were centrifuged and washed a further three times. CFSE-labeled PBMCs (1×10^5) were plated into 96-well plates in the presence of CAFs or NFs (2.5×10^4) or culture supernatants from CAFs or NFs (half-diluted with conditioned RPMI 1640 medium). An anti-CD3/anti-CD28 stimulus (Treg Suppression Inspector human; Miltenyi Biotec, Bergisch Gladbach, Germany) was added, and the incubation continued for a further 4 days. They were then harvested and washed with phosphate-buffered saline (PBS) supplemented with 0.1 % FBS and 0.1 % NaN3. They were stained with allophycocyanin (APC)-CD3 (BD Bioscience) and 7-amino-actinomycin D (7-AAD; BD Bioscience). The proliferation of T cells was analyzed by the dilution of CFSE staining intensity using flow cytometry. Viable T cells were gated based on positive CD3 staining and negative 7-AAD staining. For blocking and neutralizing experiments, anti-B7H1 mAb and anti-B7DC mAb (each 10 μg/ml; eBioscience) and anti-TGF-β mAb and anti-VEGF mAb (each 10 μg/ml; R&D Systems) were used, respectively.

T cell apoptosis assay

A total of 500,000 PBMCs obtained from healthy donors were plated onto 48-well plates in culture supernatants from CAFs or NFs (half-diluted with conditioned RPMI 1640 medium). An anti-CD3/anti-CD28 stimulus was added and the incubation continued for a further 3 days. A CaspACE™ fluorescein isothiocyanate (FITC)-VAD-FMK In Situ Marker (Promega, Madison, WI, USA) was used to detect T cell apoptosis. After 3 days, PBMCs were harvested and washed with PBS supplemented with 0.1 % FBS and 0.1 % NaN3 and then stained with FITC-VAD-FMK according to the manufacturer's instructions. They were subsequently stained with APC-CD3 (BD Bioscience) and then analyzed by flow cytometry. Five microliters of 7-AAD was added prior to flow cytometry. T cells were gated based on positive CD3 staining.

Regulatory T cell induction assay

A total of 500,000 PBMCs obtained from healthy donors were plated onto 48-well plates in culture supernatants from CAFs or NFs (half-diluted with conditioned RPMI 1640 medium). An anti-CD3/anti-CD28 stimulus was added, and the incubation continued for a further 4 days. They were then harvested and washed with PBS supplemented with 0.1 % FBS and 0.1 % NaN3. To detect Foxp3+ regulatory T cells (Tregs), cells were stained with APC-CD4 antibodies (BD Bioscience), and intracellular staining for PE-Foxp3 (eBioscience) was then performed using a Cytofix/Cytoperm™ Kit and analyzed by flow

cytometry. Incubated PBMCs were harvested and washed with PBS and analyzed according to the method described in the real-time quantitative RT-PCR section. The relative mRNA expression levels of *FOXP3*, *IL10*, and *TGFB1* were examined.

Microarray analysis and pathway analysis

Three (CAF1/NF1, CAF2/NF2, and CAF3/NF3) of six pairs were compared using Agilent Whole Human Genome Oligo Microarrays (Agilent Technologies, Santa Clara, CA) according to the manufacturer's instructions. RNA was isolated using standard RNA extraction protocols (NucleoSpin RNA II, Macherey-Nagel, Germany), and qualified with a model of the 2100 Bioanalyzer (Agilent Technologies). All samples showed RNA Integrity Numbers of greater than 6.0 (9.9–10.0) and were subjected to microarray experiments. A hundred nanograms of the RNAs from NFs and CAFs were amplified and labeled with cyanine (Cy)3 and Cy5, respectively, using the Agilent Low Input Quick Amp Labeling kit (Agilent Technologies). The hybridization procedure was performed according to the Agilent 60-mer oligo microarray processing protocol using the Agilent Gene Expression Hybridization kit (Agilent Technologies). Briefly, 300 ng of the corresponding Cy3- and Cy5-labeled fragmented cRNA was combined and hybridized to the Agilent Whole Human Genome Oligo Microarray 8x60 k V2, and the fluorescence signals of the hybridized Agilent oligo microarrays were detected using Agilent's DNA microarray scanner (Agilent Technologies). The Agilent Feature Extraction Software was used to read out and process the microarray image files. The commonly upregulated genes (cutoff value, log 10 (ratio) > 0.5) in the three pairs were used for the pathway analysis using Ingenuity Pathway Analysis (IPA) software (Ingenuity Systems).

Statistical analysis

The Wilcoxon signed-rank test was used to test for differences in the means between two groups. Two-sided P values <0.05 were considered to be significant. All statistical analyses were performed using the Statistical Package for the Social Sciences version 22.0 (SPSS, Armonk, NY).

Results

Establishment of CAFs and NFs from HNSCC

Six pairs of CAFs and NFs were generated from the resected tumor samples of patients with HNSCC. These cells grew in primary cultures in an adherent fashion and possessed a fibroblast-like morphology. To confirm that these cells were fibroblasts, and not contaminated with leukocytes, endothelial cells, and tumor cells, cells were analyzed using flow cytometry. As shown in Fig. 1a, NFs and CAFs were both negative for CD11b, CD34, and CD45, and positive for CD90 and FAP, which indicated that they were not contaminated by any other cells. The levels of α-SMA expressed by CAFs were higher than those by NFs, indicating that fibroblasts prepared from tumor tissues possessed an activated phenotype. These results confirmed the identity of the cultures as CAFs and NFs for further assays.

Expression of HLA molecules and co-regulatory molecules on CAFs and NFs

The expression of HLA molecules and B7 family co-regulatory molecules was investigated to characterize the immunological phenotypes of CAFs and NF. CAFs and NFs were both positive for HLA class I, but not for HLA-DR, and the expression level of HLA class I was similar between CAFs and NFs (data not shown). As shown in Fig. 1b, CAFs and NFs were both negative for CD80, CD86, and B7H3. Furthermore, CAFs, but not NFs, expressed B7H1 and B7DC on the cell surface; however, the expression level of B7H1 and B7DC on CAFs was modest.

Up-regulation of cytokine genes in CAFs

We analyzed differences in the expression levels of various cytokine genes, including *IL6*, *CXCL8*, *TNF*, *TGFB1*, and *VEGFA*, between CAFs and NFs by real-time quantitative RT-PCR. The expression levels of the cytokine genes tested were higher in CAFs obtained from six HNSCC patients than in control NFs (Fig. 1c). Their increasing ratio of gene expression varied with each cytokine or in each case.

Inhibition of T cell proliferation

To assess the effects of CAFs and NFs on T cell proliferation, CAFs and NFs were co-cultured with CFSE-labeled T cells. After 4 days of being co-cultured with the anti-CD3/anti-CD28 stimulus, the proliferation of T cells was measured using flow cytometry. In co-cultures, the suppressor activity of CAFs was greater than that of NFs (Fig. 2a). In order to confirm whether CAFs suppressed T cell proliferation in a cell contact-dependent or cytokine-dependent manner, the culture supernatant from CAFs was harvested and used instead of CAFs in the T cell proliferation assay. As expected, the inhibition of T cell proliferation by the culture supernatant from CAFs was higher than that from NFs (Fig. 2b). Moreover, as shown in Fig. 2c, in six HNSCC patients tested, the culture supernatant from CAFs showed greater suppressor activity than that from NFs. These results suggested that CAFs directly suppressed

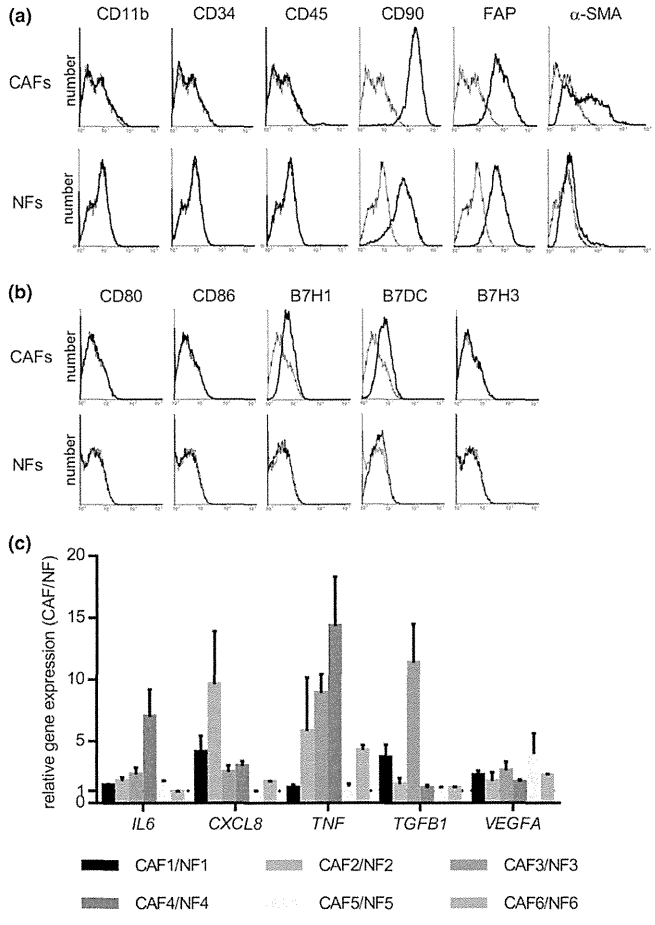

Fig. 1 Establishment of CAFs and NFs from HNSCC and their characteristics. Flow cytometry analysis of CAFs and NFs generated from resected tumor samples of patients with HNSCC. Primary cultures of CAFs and NFs were stained with CD11b, CD34, CD45, CD90, FAP, and α-SMA. CAFs and NFs were both negative for CD11b, CD34, and CD45, and positive for CD90 and FAP. α-SMA expression levels in CAFs were higher than those in NFs. **a** Representative data from one cancer patient. The expression of co-stimulatory and co-regulatory molecules on CAFs and NFs. Flow cytometry was performed as described in the "Materials and methods" section. **b** Representative data from one cancer patient. CAFs and NFs were both negative for CD80, CD86, and B7H3. The expression levels of B7H1 and B7DC in CAFs were higher than those in NFs. Up-regulation of cytokine genes in CAFs from HNSCC patients. **c** Total RNA was extracted from the generated CAFs and NFs, and increases in the expression levels of *IL6*, *CXCL8*, *TNF*, *TGFB1*, and/or *VEGFA* were detected by real-time qRT-PCR

anti-tumor immune responses by producing various soluble factors including immunosuppressive cytokines.

Inhibitory mechanisms of T cell proliferation by CAFs

Next, the potential role of co-regulatory molecules and immunosuppressive cytokines in the suppressive function of CAFs was investigated through the use of mAbs. As expected, addition of anti-B7H1 mAb and anti-B7DC mAb significantly restored T cell proliferation (Fig. 3a, b). Thus, the suppressive effects of CAFs appear to be partially mediated by co-regulatory molecules. These results suggested that CAFs had different immunological properties to NFs. Similarly, we investigated the importance of two immunosuppressive cytokines, TGF-β and VEGF, as key molecules suppressing T cell proliferation. To end this, we neutralized TGF-β and VEGF from supernatants of CAFs using antibodies. As shown in Fig. 3c, d, neutralizing TGF-β and VEGF led to an increase of proliferated T cells. These findings suggest a pivotal role of TGF-β and VEGF as soluble factors in immune suppression mediated by CAFs.

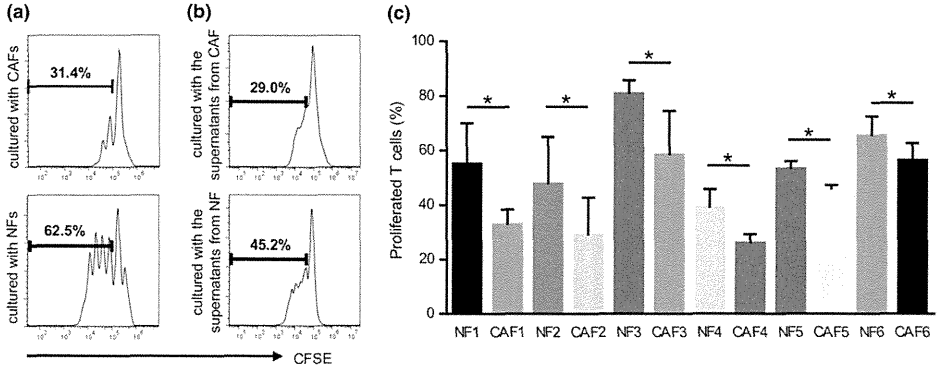

Fig. 2 Suppressive activity on T cell proliferation by CAFs and NFs. Generated CAFs and NFs were co-cultured with CFSE-labeled T cells for 4 days with an anti-CD3/anti-CD28 stimulus. They were stained with APC-CD3 and 7-amino-actinomycin D (7-AAD) to gate viable CD3+ T cells. The proliferation of T cells was analyzed by the reduction of CFSE staining intensity using flow cytometry. **a** Representative data of the proliferation of T cells cultured with CAFs or NFs. **b** Representative data of the proliferation of T cells cultured with supernatants from CAFs or NFs. **c** The culture supernatant from CAFs showed greater suppressor activity than that from NFs in six HNSCC patients tested. Bars indicate mean values derived from 6 independent experiments. *Asterisk* indicates significant difference ($P < 0.05$) between NFs and CAFs

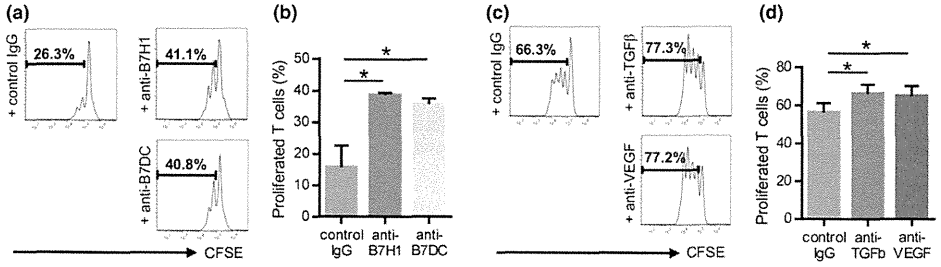

Fig. 3 Role of co-regulatory molecules and immunosuppressive cytokines in T cell suppression by CAFs. CAFs were pretreated with anti-B7H1 mAb or anti-B7DC mAb, and then co-cultured with CFSE-labeled T cells for 4 days with an anti-CD3/anti-CD28 stimulus. The proliferation of T cells was analyzed using flow cytometry. **a** Representative data from one patient (CAF5). **b** Addition of anti-B7H1 mAb and anti-B7DC mAb significantly restored T cell proliferation. Similarly, CAFs supernatants were pretreated with anti-TGF-β or anti-VEGF neutralizing mAb, and then added to CFSE-labeled PBMCs for T cell proliferation assays. **c** Representative data from one patient (CAF3). **d** TGF-β and VEGF neutralization also significantly increased the percentage of proliferated T cells. *Asterisk* indicates significant difference ($P < 0.05$) compared with control IgG

Induction of T cell apoptosis

To further elucidate the mechanisms underlying the suppression of T cell proliferation, we investigated whether the culture supernatants obtained from CAFs and NFs induced T cell apoptosis. Healthy donor PBMCs were cultured with supernatants from CAFs or NFs for 3 days with an anti-CD3/anti-CD28 stimulus, and were subsequently analyzed by flow cytometry. The proportions of apoptotic T cells in PBMCs co-cultured with the supernatant from CAFs were significantly higher than those co-cultured with the supernatant from NFs (Fig. 4a, b).

Induction of regulatory T (Treg) cells

We compared the percentages of Treg cells in PBMCs co-cultured with supernatant obtained from CAFs or NFs. Representative dot plots of Treg cells

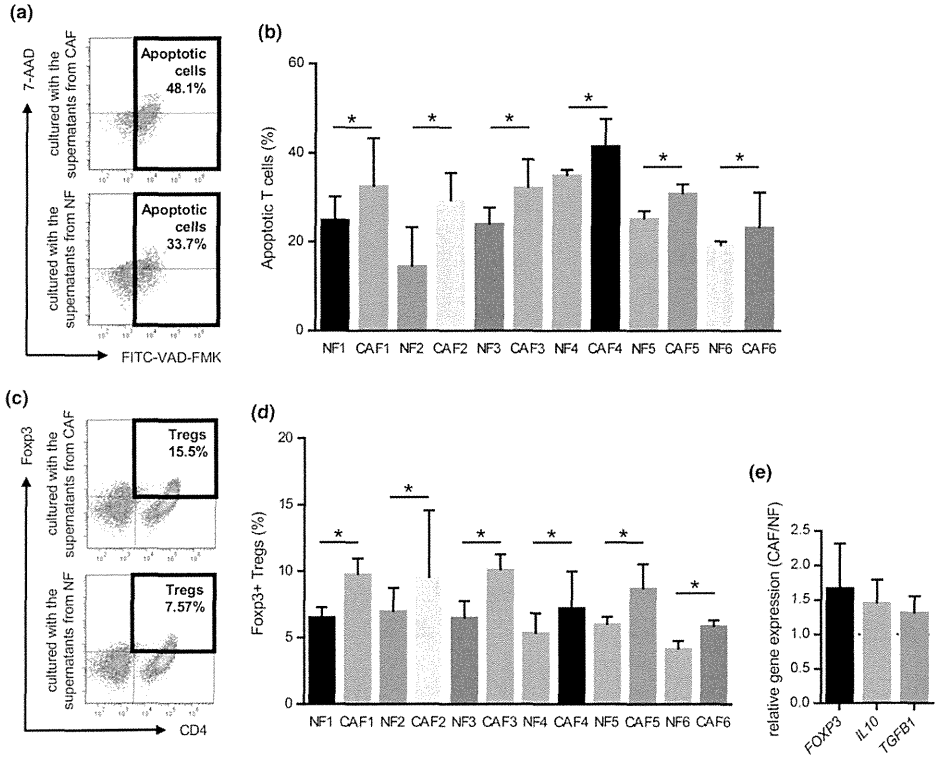

Fig. 4 Induction of T cell apoptosis and Treg (CD4+Foxp3+) in PBMCs co-cultured with the supernatant from CAFs or NFs. PBMCs prepared from healthy donors were cultured with the supernatant from CAFs or NFs for 3 days with an anti-CD3/anti-CD28 stimulus, and subsequently analyzed by flow cytometry. They were stained with FITC-VAD-FMK, APC-CD3, and 7-amino-actinomycin D (7-AAD), and CD3+ T cells were gated. **a** Representative data of apoptotic T cells cultured with CAFs or NFs. **b** The induction of T cell apoptosis was significantly greater by CAFs from the six HNSCC patients tested than by NFs. Bars indicate mean values derived from 6 independent experiments. *Asterisk* indicates significant difference ($P < 0.05$) between NFs and CAFs. PBMCs prepared from healthy donors were co-cultured with the supernatant from CAFs or NFs for 4 days with an anti-CD3/anti-CD28 stimulus. They were stained with PE-Foxp3 and APC-CD4, and then analyzed by flow cytometry. They were also analyzed by real-time qRT-PCR after a 3-day incubation. **c** Representative data of CD4+Foxp3+Tregs in PBMCs co-cultured with the supernatant from CAFs or NFs. **d** The induction of T reg was significantly greater by CAFs from the six HNSCC patients tested than by NFs. Bars indicate mean values derived from 6 independent experiments. *Asterisk* indicates significant difference ($P < 0.05$) between NFs and CAFs. **e** The expression levels of Treg-related genes including *FOXP3*, *TGFB1*, and *IL10* in PBMCs co-cultured with the supernatant from CAFs was higher than those co-cultured with the supernatant from with NFs

(CD4+FOXP3+) are shown in Fig. 4c. As expected, the proportions of Treg cells in PBMCs co-cultured with the supernatant obtained from CAFs were significantly higher than those co-cultured with the supernatant from NFs (Fig. 4d). Moreover, the gene expression levels of the Treg-specific transcription factors *FOXP3*, *IL-10*, and *TGFB1* in PBMCs co-cultured with supernatant were analyzed by real-time quantitative RT-PCR, and the expression levels of *FOXP3*, *IL10*, and *TGFB1* were higher in PBMCs co-cultured with supernatant obtained from CAFs than in those co-cultured with the supernatant from NFs (Fig. 4e). These results suggested that CAFs also indirectly suppressed anti-tumor immune responses by inducing Treg cells.

Microarray analysis and pathway analysis

We performed Agilent Whole Human Genome Microarray analyses with the three pairs of CAFs and NFs. Although a hierarchical cluster analysis from the three (CAF1/NF1, CAF2/NF2, and CAF3/NF3) of six pairs revealed different genetic profiles, as shown in Fig. 5a, a hundred genes that were upregulated in the three CAFs (log 10 ratio > 0.5) were identified (Fig. 5b). To explore the altered canonical pathways in CAFs from those in NFs, we characterized the functional relationship between genes upregulated in CAFs in IPA. Two signaling pathways, the leukocyte extravasation and paxillin signaling pathways, have been predicted as the most significantly activated canonical pathways (Table 1).

Discussion

Anti-tumor immunity has been considered to play an important role in protecting against the development of malignancy. The immune system monitors and excludes tumor cells in the early phase of tumorigenesis, and fibroblasts also contribute to a growth suppressive state, while tumor cell variants show increased resistance to immune surveillance and gradually survive and proliferate. Immune responses against tumor cells in the TME were previously reported to be strongly suppressed through a dysfunction in effector cells, as well as the infiltration and expansion of immune suppressive cells, and where fibroblasts educated by tumor cells become CAFs contributing to tumorigenesis, tumor growth, and metastasis [5, 9]. Regarding the contribution of CAFs to immune evasion, Balsamo et al. [17] demonstrated that CAFs from melanoma interfered with NK cell functions including cytotoxicity and cytokine production. On the other hand, De Monte et al. [18] reported that CAFs from pancreatic cancer induced thymic stromal lymphopoietin-dependent Th2-type inflammation. In addition to these findings, we were able to demonstrate in the present study that CAFs obtained from HNSCC were of unique immunological significance, as opposed to NFs.

Our results revealed that CAFs suppressed T cell proliferation more efficiently than NFs. This suppressive activity was observed in co-cultures not only with CAFs, but also the supernatant from CAFs. To elucidate the mechanisms underlying the suppressive effects of CAFs on T cell proliferation, we first assessed the expression of co-stimulatory and co-regulatory molecules by CAFs and NFs. Although co-stimulatory molecules, CD80 and CD86, were not expressed by CAFs or NFs, B7H1 and B7DC were expressed by CAFs, but not by NFs. B7H1 and B7DC are both members of the B7 family, bind PD-1 on activating T cells, and are putative negative regulators for immune function. Nazareth et al. [19] demonstrated that a subset of CAFs obtained from non-small cell lung cancer (NSCLC) constitutively expressed B7H1 and B7DC. The intensity of B7H1/B7DC expression in CAFs from HNSCC was more modest than that in CAFs obtained from NSCLC. We performed blocking assays using anti-B7H1 and anti-B7DC mAbs, and suppressive activity was significantly restored in some of pairs tested. Nazareth et al. showed that the blockade of B7H1 and/or B7DC completely reversed the inhibition of tumor-associated T cell activation by CAFs in one of three tumors. Thus, our results and previous findings suggest that co-regulatory molecules on CAFs may partially play an important role in T cell suppression. CAFs originally consist of a heterogeneous population of cells from various sources; therefore, the role of B7H1 and B7/DC expression in CAFs may vary depending on factors such as their functional activities, types of cancers, and immune status in the TME. Several monoclonal antibodies that target B7H1 (PD-L1) are now being developed [20, 21], and the blockade of B7H1 was recently shown to produce durable tumor regression and prolonged disease stabilization in patients with advanced cancers in a phase I trial [22]. Monoclonal antibodies against co-regulatory molecules may be somewhat useful as a CAF-targeted therapy.

Since CAFs suppressed T cell proliferation in a contact-independent manner, we investigated T cell apoptosis and Treg induction using culture supernatants from CAFs and NFs in order to elucidate the suppression mechanisms responsible in more detail. Previous studies have so far demonstrated that CAFs produce various cytokines and/or chemokines to promote tumor cell proliferation, angiogenesis, invasion, and metastatic dissemination [9]. Several studies found that CAFs isolated from HNSCC expressed higher levels of hepatocyte growth factor (HGF) [23], TGF-β [24], IL-33 [25], chemokine ligand 7 (CCL7) [26], and matrix metalloproteinase (MMP) [27] than their normal counterparts. We also revealed that the gene expression levels of *IL6*, *CXCL8*, *TNF*, *TGFB1*, and *VEGFA* were higher in CAFs than in NFs. Among the cytokines evaluated in the present study, TNF-α is known to be a member of cytokines that induce apoptotic cell death in T cells. Therefore, it was not unexpected to find that CAFs significantly induced T cell apoptosis; however, difficulties have been associated with determining the exact factors involved in T cell apoptosis due to its complicated composition. PBMCs co-cultured with the supernatant from CAFs preferentially induced Treg. Moreover, the gene expression levels of *FOXP3*, *TGFB1*, and *IL10* were elevated in PBMCs co-cultured with the supernatant from CAFs, which supported the induced Treg being functionally activated. Treg has been shown to accumulate in the TME, promote tumor growth, and down-regulate anti-tumor responses [28]. The differentiation of precursor T cells is regulated by a complex network of specific cytokine signals, and a certain type of Treg is known to be induced in the

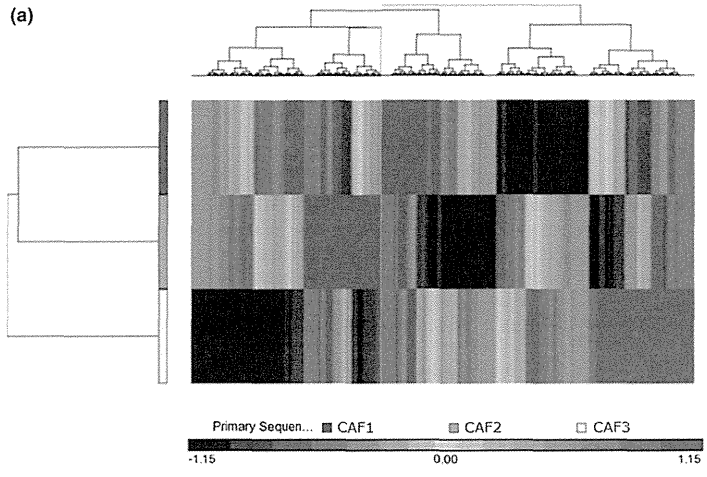

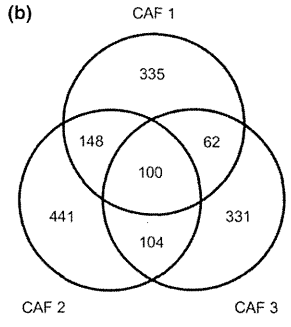

ST6GALNAC5	*IL17F*	*PDZRN4*	*MBOAT1*	*PROC*
NFE2L3	*BST2*	*COL8A1*	*TFAP2A*	*NXPH2*
APCDD1	*RAB38*	*DMD*	*CD163L1*	*PLCB4*
TNFSF4	*TRPA1*	*GPR65*	*ADAMTS12*	*SLC24A4*
WFDC1	*STRA6*	*FAM169A*	*PAGE3*	*RNF144B*
VAT1L	*MAMDC2*	*COLEC10*	*CLDN18*	*MIR143HG*
SLC24A3	*OR10A7*	*MC5R*	*VWC2L*	*VPREB3*
RUNX3	*NEDD9*	*OR9G4*	*PSG1*	*KIAA0408*
LEF1	*ITGA1*	*SGIP1*	*CLDN1*	*ITGA4*
C7orf69	*TMEM176B*	*PYY*	*GREB1L*	*STYK1*
COL10A1	*B3GALT2*	*DMRT1*	*LINC00483*	*FRY*
BEX1	*ELOVL2*	*LINC00460*	*PSG8*	*NRXN1*
EFNB2	*CHN1*	*RASGRP1*	*FOLH1*	*PNKD*
NTF3	*AZU1*	*CLEC1A*	*CD8A*	*LINC00161*
FAM155A	*MMP1*	*HCLS1*	*TNS3*	*LRRC38*
HSPA2	*PADI1*	*MRVI1*	*SHROOM2*	*BCL11B*
PTPRB	*MMP3*	*A2M*	*LYPD6*	*H2AFB3*
RASEF	*SNCAIP*	*FRZB*	*CNN1*	*AGAP6*
OXTR	*DKK2*	*ANGPT1*	*FGF1*	*LINC00862*
EML5	*FAM84A*	*FAM101A*	*PIK3R3*	*RGCC*

Fig. 5 Microarray analyses with the three pairs of CAFs and NFs. **a** Cluster diagram of a microarray analysis from three pairs of NFs and CAFs. The color bar estimates relative expression levels: *Red* indicates higher than average expression and blue indicates lower than average expression. **b** A list of commonly upregulated genes in CAFs obtained from three patients with HNSCC. A total of one hundred genes were identified as commonly upregulated genes from the microarray analysis between NFs and CAFs. The cutoff value of the log 10 (ratio) was set to be greater than 0.5

periphery in response to IL-2, TGF-β, and IL-10 [29]. Moreover, VEGF has been recognized as an important factor in the induction or maintenance of Treg [30]. The up-regulation of *TGFB1* and *VEGFA* in CAFs may play an important role in the induction of Treg. In fact, restoration of T cell proliferation by TGF-β and VEGF neutralization in the present

Table 1 List of genes in significantly upregulated canonical pathways identified by IPA

Ingenuity canonical pathways	Sample	−log (*P* value)	Ratio	z-Score	Molecules
Leukocyte extravasation signaling	Pt-1	5.70	0.104	3.5	*RAC2,VCAM1,ICAM1,MMP3,ACTN3,CLDN18,ITGA6,ITGB3, PIK3R3, ITGB2,ITGA3,EDIL3,ARHGAP9, ACTA2,CLDN1,RASGRP1,ITGA1, CLDN9,MMP1,ITGA4*
	Pt-2	5.80	0.119	3.771	*MMP3,ACTB,ACTN3,CLDN18, ITGA6,PIK3R3,ITGB2,CLDN24, ITGA3,EDIL3,ACTA2,ARHGAP9, CLDN1,PLCG2,RASGRP1,ITGA1, ACTG2,CLDN9,MMP12,ACTN1, MMP1,ATM,ITGA4*
	Pt-3	4.51	0.088	3.317	*CLDN11,SPN,MMP3,CLDN18,JAM2,MMP25,CLDN6,MMP27 ,PIK3R3, CLDN1,RASGRP1,PIK3R6,ITGA1, ACTG2,MMP12,MMP1,ITGA4*
Paxillin signaling	Pt-1	2.51	0.092	2.236	*PIK3R3,ITGB2,ITGA3,ACTA2, ACTN3,ITGA6,ITGA1,ITGA4,ITGB3*
	Pt-2	3.42	0.122	3	*PIK3R3,ITGB2,ITGA3,ACTA2,ACTB,ACTN3,ITGA6,ITGA1,A CTG2, ACTN1,ITGA4,ATM*
	Pt-3	1.70	0.071	2.449	*PIK3R3,PAK3,ARHGEF7,PIK3R6, ITGA1,ACTG2,ITGA4*

study supports that. Mace et al. [31] similarly demonstrated that a culture of PBMCs with pancreatic cancer stellate cell supernatants promoted PBMC differentiation into myeloid-derived suppressor cells, which is another major subset of regulatory cells, in a STAT3-dependent manner. Thus, various factors secreted by CAFs appear to act synergistically or additively to enhance immunosuppressive ability, leading to a dysfunction in effector T cells.

We also compared the gene expression profiles of CAFs and NFs using a microarray analysis. The hierarchical clustering of gene expression in CAFs than in NFs clearly showed differences between individual patients. These results suggest that the characteristics of CAFs in the TME may be regulated by various conditions, such as inflammation, hypoxia, and angiogenesis, in which CAFs exist. In order to elucidate the activated signaling pathway related to CAFs, commonly upregulated genes in the three pairs were analyzed with IPA. Although any signaling pathway related to immunosuppression was not detected in this study, we additionally found that a set of genes, the expression of which was upregulated in CAFs, were involved in the leukocyte extravasation and paxillin signaling pathways. Paxillin is one of the crucial molecules for cell–extracellular matrix adhesion and cell migration, and plays an important role in the assembly and disassembly of focal adhesions in various cells [32, 33]. These activated signaling pathways in CAFs may facilitate the recruitment of various leukocytes including immunosuppressive cells in the TME.

In summary, we established pairs of CAFs and NFs from patients with HNSCC. CAFs expressed not only the co-regulatory molecules, B7H1 and B7DC, but also preferentially induced T cell apoptosis and Treg over NFs. Moreover, the leukocyte extravasation and paxillin signaling pathways were predicted to be the most significantly activated canonical pathways in CAFs relative to those in NFs. Thus, CAFs modulated effector T cell function in anti-tumor immune responses in direct and indirect manners. Tumor evasion from the host immune system is a major problem in immunotherapy, and CAFs may play a pivotal role in the TME by establishing an immunosuppressive network along with tumor cells and immunosuppressive cells that facilitates the activation of an immunosuppressive pathway. Accordingly, the development of novel therapeutic agents to efficiently overcome CAF-driven immunosuppression is urgently needed.

Acknowledgments This work was supported in part by KAKENHI (Grants-in-Aid for Scientific Research) (15K10798 to Koichi Sakakura, 25861525 to Minoru Toyoda, 26670736 to Kazuaki Chikamatsu). We thank Dr. Theresa L. Whiteside for her critical reading and comments.

Compliance with ethical standards

Conflict of interest The authors declare that they have no conflict of interest.

References

1. Siegel R, Naishandham D, Jemal A (2012) Cancer statistics, 2012. CA Cancer J Clin 62:10–29

2. Leemans CR, Braakhuis BJM, Brakenhoff RH (2011) The molecular biology of head and neck cancer. Nat Rev Cancer 11:9–22
3. Augsten M (2014) Cancer-associated fibroblasts as another polarized cell type of the tumor microenvironment. Front Oncol 4:62
4. Franco OE, Shaw AK, Strand DW, Hayward SW (2010) Cancer associated fibroblasts in cancer pathogenesis. Semin Cell Dev Biol 21:33–39
5. Kalluri R, Zeisberg M (2006) Fibroblasts in cancer. Nat Rev Cancer 6:392–401
6. Ito M, Ishii G, Nagai K, Maeda R, Nakano Y, Ochiai A (2012) Prognostic impact of cancer-associated stromal cells in patients with stage I lung adenocarcinoma. Chest 142:151–158
7. Herrera M, Herrera A, Domínguez G, Silva J, García V, García JM, Gómez I, Soldevilla B, Muñoz C, Provencio M, Campos-Martin Y, García de Herreros A et al (2013) Cancer-associated fibroblast and M2 macrophage markers together predict outcome in colorectal cancer patients. Cancer Sci 104:437–444
8. Zhang J, Liu J (2013) Tumor stroma as targets for cancer therapy. Pharmacol Ther 137:200–215
9. Rasanen K, Vaheri A (2010) Activation of fibroblasts in cancer stroma. Exp Cell Res 316:2713–2722
10. Zhang L, Conejo-Garcia JR, Katsaros D, Gimotty PA, Massobrio M, Regnani G, Makrigiannakis A, Gray H, Schlienger K, Liebman MN, Rubin SC, Coukos G (2003) Intratumoral T cells, recurrence, and survival in epithelial ovarian cancer. N Engl J Med 348:203–213
11. Pages F, Berger A, Camus M, Sanchez-Cabo F, Costes A, Molidor R, Mlecnik B, Kirilovsky A, Nilsson M, Damotte D, Meatchi T, Bruneval P et al (2005) Effector memory T cells, early metastasis, and survival in colorectal cancer. N Engl J Med 353:2654–2666
12. Whiteside TL (2010) Immune responses to malignancies. J Allergy Clin Immunol 125:S272–S283
13. Talmadge JE (2011) Immune cell infiltration of primary and metastatic lesions: mechanisms and clinical impact. Semin Cancer Biol 21:131–138
14. Poschke I, Mougiakakos D, Kiessling R (2011) Camouflage and sabotage: tumor escape from the immune system. Cancer Immunol Immunother 60:1161–1171
15. Hanahan D, Weinberg RA (2011) Hallmarks of cancer: the next generation. Cell 144:646–674
16. Tong CCL, Kao J, Silora AG (2012) Recognizing and reversing the immunosuppressive tumor microenvironment of head and neck cancer. Immunol Res 54:266–274
17. Balsamo M, Scordamaglia F, Pietra G, Manzini C, Cantoni C, Boitano M, Queirolo P, Vermi W, Facchetti F, Moretta A, Moretta L, Mingari MC et al (2009) Melanoma-associated fibroblasts modulate NK cell phenotype and antitumor cytotoxicity. Proc Natl Acad Sci USA 106:20847–20852
18. De Monte L, Reni M, Tassi E, Clavenna D, Papa I, Recalde H, Braga M, Di Carlo V, Doglioni C, Protti MP (2011) Intratumor T helper type 2 cell infiltrate correlates with cancer-associated fibroblast thymic stromal lymphopoietin production and reduced survival in pancreatic cancer. J Exp Med 208:469–478
19. Nazareth MR, Broderick L, Simpson-Abelson MR, Kelleher RJ Jr, Yokota SJ, Bankert RB (2007) Characterization of human lung tumor-associated fibroblasts and their ability to modulate the activation of tumor-associated T cells. J Immunol 178:5552–5562
20. Kyi C, Postow MA (2014) Checkpoint blocking antibodies in cancer immunotherapy. FEBS Lett 588:368–376
21. Hamid O, Carvajal RD (2013) Anti-programmed death-1 and anti-programmed death-ligand 1 antibodies in cancer therapy. Expert Opin Biol Ther 13:847–861
22. Brahmer JR, Tykodi SS, Chow LQ, Hwu WJ, Topalian SL, Hwu P, Drake CG, Camacho LH, Kauh J, Odunsi K, Pitot HC, Hamid O et al (2012) Safety and activity of anti-PD-L1 antibody in patients with advanced cancer. N Engl J Med 366:2455–2465
23. Knowles LM, Stabile LP, Egloff AM, Rothstein ME, Thomas SM, Gubish CT, Lerner EC, Seethala RR, Suzuki S, Quesnelle KM, Morgan S, Ferris RL et al (2009) HGF and c-Met participate in paracrine tumorigenic pathways in head and neck squamous cell cancer. Clin Cancer Res 15:3740–3750
24. Rosenthal E, McCrory A, Talbert M, Young G, Murphy-Ullrich J, Gladson C (2004) Elevated expression of TGF-β1 in head and neck cancer-associated fibroblasts. Mol Carcinog 40:116–121
25. Chen SF, Nieh S, Jao SW, Wu MZ, Liu CL, Chang YC, Lin YS (2013) The paracrine effect of cancer-associated fibroblast-induced interleukin-33 regulates the invasiveness of head and neck squamous cell carcinoma. J Pathol 231:180–189
26. Jung DW, Che ZM, Kim J, Kim K, Kim KY, Williams D, Kim J (2010) Tumor-stromal crosstalk in invasion of oral squamous cell carcinoma: a pivotal role of CCL7. Int J Cancer 127:332–344
27. Johansson AC, Ansell A, Jerhammar F, Lindh MB, Grenman R, Munck-Wikland E, Östman A, Roberg K (2012) Cancer-associated fibroblasts induce matrix metalloproteinase-mediated cetuximab resistance in head and neck squamous cell carcinoma cells. Mol Cancer Res 10:1158–1168
28. Elkord E, Alcantar-Orozco EM, Dovedi SJ, Tran DQ, Hawkins RE, Gilham DE (2010) T regulatory cells in cancer: recent advances and therapeutic potential. Expert Opin Biol Ther 10:1573–1586
29. Knosp CA, Johnston JA (2012) Regulation of CD4+ T-cell polarization by suppressor of cytokine signalling proteins. Immunology 135:101–111
30. Wada J, Suzuki H, Fuchino R, Yamasaki A, Nagai S, Yanai K, Koga K, Nakamura M, Tanaka M, Morisaki T, Katano M (2009) The contribution of vascular endothelial growth factor to the induction of regulatory T-cells in malignant effusions. Anticancer Res 29:881–888
31. Mace TA, Ameen Z, Collins A, Wojcik S, Mair M, Young GS, Fuchs JR, Eubank TD, Frankel WL, Bekaii-Saab T, Bloomston M, Lesinski GB (2013) Pancreatic cancer-associated stellate cells promote differentiation of myeloid-derived suppressor cells in a STAT3-dependent manner. Cancer Res 73:3007–3018
32. Gumbiner BM (1996) Cell adhesion: the molecular basis of tissue architecture and morphogenesis. Cell 84:345–357
33. Turner CE (2000) Paxillin and focal adhesion signaling. Nat Cell Biol 2:E231–E236